Vol 17 No 1, January 2008
1674-1056/2008/17(01)/0211-06

Chinese Physics B

© 2008 Chin. Phys. Soc.
and IOP Publishing Ltd

Continuous-wave mid-infrared intracavity singly resonant optical parametric oscillator based on periodically poled lithium niobate*

Ding Xin(丁 欣)[a)b)c)†], Zhang Shao-Min(张少敏)[a)b)c)], Ma Hong-Mei(马洪梅)[a)b)c)], Pang Ming(庞 明)[a)b)c)], Yao Jian-Quan(姚建铨)[a)b)c)], and Li Zhuo(李 卓)[d)]

[a)] *College of Precision Instrument and Opto-Electronics Engineering, Institute of Laser and Opto-Electronics, Tianjin University, Tianjin* 300072, *China*
[b)] *Key Laboratory of Opto-Electronics Information Science and Technology, Ministry of Education, Tianjin* 300072, *China*
[c)] *Cooperated Institute of Nankai University and Tianjin University, Tianjin* 300072, *China*
[d)] *School of Information Science and Technology, Department of Opto-Electronic Engineering, Beijing Institute of Technology, Beijing* 100081, *China*

(Received 11 April 2007; revised manuscript received 15 May 2007)

This paper reports a continuous-wave (CW) mid-infrared intracavity singly resonant optical parametric oscillator based on periodically poled lithium niobate (PPLN) pumped by a diode-end-pumped CW Nd:YVO_4 laser. Considering the thermal lens effects, it adopted an optical ballast lens and the near-concentric cavity for better operation. At the PPLN's grating period of 28.5 μm and the temperature of 140°C, the maximum idler output power of 155 mW at 3.86 μm has been achieved when the 808 nm pump power is 8.5 W, leading to an optical-to-optical conversion efficiency of 1.82%.

Keywords: continuous-wave, mid-infrared, intracavity optical parametric oscillator, periodically poled lithium niobate crystal

PACC: 4265K, 4265, 4260

1. Introduction

3–5 μm waves are desirable in various applications including laser spectrum, atmospheric pollution monitor, remote detection, differential absorption lidar (DIAL) and time-resolved spectroscopy of semi-conductors and so on. Optical parametric oscillators (OPOs) are attractive all-solid-state sources for generating mid-infrared waves. Recently, a number of mid-infrared waves based on OPOs have been reported:[1−7] Stothard *et al* reported a diode-pumped Nd:YVO_4 laser with intracavity singly resonant optical parametric oscillator (SRO) that hosts periodically poled lithium niobate (PPLN) in 1998. At 1W of input diode power, 70 mW of idler at 3.66 um, which corresponds to a photon conversion efficiency of 55%, has been achieved.[5] In 2003, an intracavity continuous-wave (CW) OPO based on $PPRbTiOAsO_4$ pumped by 1064 nm Nd:YVO_4 laser was described. When the diode-laser power is 3 W, the maximum power 65 mW of idler at 3.52 μm was obtained, indicating an optical-to-optical conversion efficiency of 2.17%.[3] In domestic fields, only the extracavity quasi-continuous-wave OPO with output wavelength at 3–5 μm have been reported.[8,9]

The OPOs are difficult in oscillating for high threshold. However, by exploiting the high circulating pump intensities, the intracavity pumping technique uniquely allows extension of the operation of CW SRO to miniature, low-threshold, low-cost, and the stable operation can be achieved without the need for cavity-length control, which are not attainable with alternative external pumping technique. In this paper, we present an intracavity CW PPLN-SRO pumped by a diode-end-pumped Nd:YVO_4 laser, which can generate CW output at 3.86 μm. The OPO threshold is only 2.1 W (diode-laser power). At the laser diode (LD) power of 8.5 W, the SRO delivers 155 mW of the maximum idler power, indicating an optical-to-optical conversion efficiency of 1.82%.

*Project supported in part by the National Natural Science Foundation of China (Grant Nos 10474071, 60637010, 60671036 and 60278001) and Tianjin Applied Fundamental Research Project, China (07JCZDJC05900).
†E-mail: dingxin@tju.edu.cn

2. CW intracavity SRO theory

2.1. Model description

Figure 1 shows a rate-equation model of the multi-mode intracavity SRO.[10] This device comprises a pump laser source, and an OPO resonator in which the signal field is resonant and the idler field exists after a single pass. The laser and OPO cavities share a common end mirror and are separated by a beam splitter (BS). A nonlinear crystal of length l is placed in the common arm, and to simplify the model, the cavities and crystal share a common end at $z = 0$.

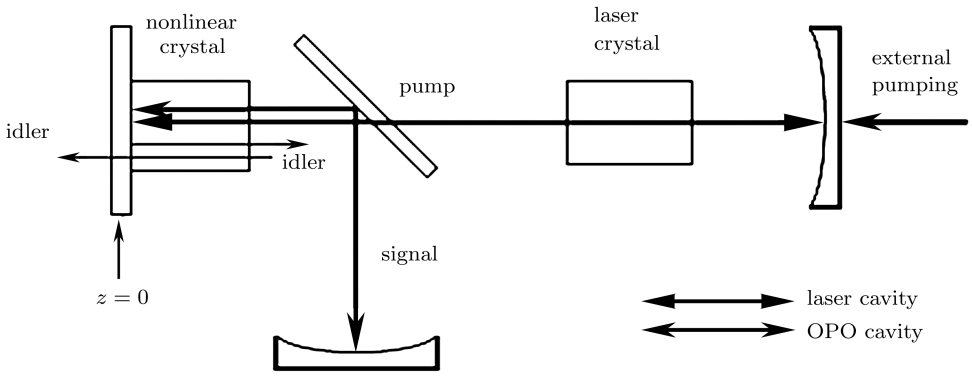


Fig.1. The theoretical model of the multi-mode intracavity SRO.

In this model, the laser bandwidth is assumed to be well within the spectral acceptance bandwidth of the parametric interaction, allowing all laser modes to couple with a single-frequency resonant signal.[11]

2.2. The laser, signal and idler fields

The laser and signal fields and the polarization generated by three interacting fields mixing are:

$$E_{\rm p}(z,r,t) = \sum_j 2E_{{\rm p}j}(t)\exp(-r^2/w_{\rm p}^2) \times \sin(k_{{\rm p}j}z)\times\cos(\omega_{{\rm p}j}t+\phi_{{\rm p}j}), \quad (1)$$

$$E_{\rm s}(z,r,t) = 2E_{\rm s}(t)\exp(-r^2/w_{\rm s}^2) \times \sin(k_{\rm s}z)\cos(\omega_{\rm s}t+\phi_{\rm s}), \quad (2)$$

$$\wp_{\rm i,s,p} = 2\varepsilon(2d_{\rm eff})E_{\rm p,i,s}(z,r,t)E_{\rm s,p,i}(z,r,t). \quad (3)$$

Here, the subscript j denotes the jth laser mode, $k_{{\rm p}j,{\rm s}} = n_{\rm p,s}\omega_{{\rm p}j,{\rm s}}/c$, and $n_{\rm p,s}$ is an effective refractive index. $w_{\rm p}$ and $w_{\rm s}$ are the laser and signal transverse waist radius in the nonlinear crystal respectively.

Only the travelling-wave components propagating in the same direction interact, and we only retain the terms satisfying $\omega_{{\rm p}j} = \omega_{\rm s}+\omega_{ij}$. The idler polarization $\wp_{\rm i}(z,r,t) = \wp_{\rm i}^{+}(z,r,t)+\wp_{\rm i}^{-}(z,r,t)$ radiates a two-way, single-pass idler field, whose axial amplitude variation is calculated from the relation

$$\frac{n_{\rm i}}{c}\frac{\partial E_{\rm i}^{\pm}(z,r,t)}{\partial t} \pm \frac{\partial E_{\rm i}^{\pm}(z,r,t)}{\partial z} = -\omega_{\rm i}\wp_{\rm i}^{\pm}(z,r,t)/(2\varepsilon_0 n_i c). \quad (4)$$

The $\pm$ distinguishes travelling waves with $\pm k_{{\rm i}j}z$. Since the idler experiences quasi-constant nonlinear source term over its transit of the crystal, the idler's temporal variations follow those of the resonant waves.[12]

For $E_{\rm i}^{\pm}(z,r,t) = 0$ at the start of each pass of the nonlinear crystal, the nonlinear coupling always fixes a phase of $\Delta\phi_j^{\pm} = \pi/2$. Setting $\Delta k = 0$ (Δk represents every value of $\Delta k_j = k_{{\rm p}j} - k_{\rm s} - k_{{\rm i}j}$ because the laser bandwidth is much smaller than the parametric gain bandwidth), combining Eqs.(1)–(4), we can simplify the idler field to:

$$E_{\rm i}^{\pm}(z,r,t) = \frac{2d_{\rm eff}}{n_{\rm i}c}\times\exp(-r^2(w_{\rm p}^{-2}+w_{\rm s}^{-2}))E_{\rm s}(t)\begin{pmatrix} z \\ l-z\end{pmatrix} \times\sum_j\{\omega_{{\rm i}j}E_{{\rm p}j}(t)\cos(-(\omega_{{\rm i}j}t+\phi_{{\rm i}j}^{\pm})\pm k_{{\rm i}j}z)\}. \quad (5)$$

The envelope of $E_{\rm i}^{\pm}(z,r,t)$ in the crystal increases linearly with $\pm z$.

2.3. The dynamical characteristics of intracavity SRO

The evolution of the resonant fields is described by the self-consistency equations:

$$\dot{E}_{\rm s}(t) + E_{\rm s}(t)/\tau_s' = -\omega_{\rm s}C_{\rm s}(t)/(2\varepsilon_0 n_s^2), \quad (6)$$

$$\dot{E}_{\mathrm{p}j}(t)+E_{\mathrm{p}j}(t)/\tau'_{\mathrm{p}} = -\omega_{\mathrm{p}j}C_{\mathrm{p}j}(t)/2\varepsilon_0 n_{\mathrm{p}}^2 - \omega_{\mathrm{p}j}\wp_{\mathrm{laser}j}(t)/(2\varepsilon_0 n_{\mathrm{p}}^2). \quad (7)$$

Here τ'_{s}, τ'_{p} are the signal- and pump-field cavity lifetimes respectively. $\wp_{\mathrm{laser}j}$ represents the polarization in the laser crystal. $C_{\mathrm{s}}(t)$, $C_{\mathrm{p}j}(t)$ are polarization terms describing the nonlinear crystal.

The resonant fields can be expressed as photon flows:[10]

$$F_{\mathrm{s}} = n_{\mathrm{s}}c\varepsilon_0 E_{\mathrm{s}}^2\pi w_{\mathrm{s}}^2/(4\hbar\omega_{\mathrm{s}}),$$
$$F_{\mathrm{p}j} = n_{\mathrm{p}}c\varepsilon_0 E_{\mathrm{p}j}^2\pi w_{\mathrm{p}}^2/(4\hbar\omega_{\mathrm{p}}j). \quad (8)$$

For the signal field to experience gain, the laser photon flow must exceed the threshold value

$$\left[\sum_j F_{\mathrm{p}j}\right]_{\mathrm{th}} = \frac{n_{\mathrm{p}}n_{\mathrm{s}}^2 n_{\mathrm{i}}c^2\varepsilon_0 L_{\mathrm{s}}}{\hbar\omega_{\mathrm{p}}\omega_{\mathrm{s}}\omega_{\mathrm{i}}\tau'_{\mathrm{s}}d_{\mathrm{eff}}^2 l^2}\frac{\pi(w_{\mathrm{s}}^2+w_{\mathrm{p}}^2)}{2}. \quad (9)$$

Thus the threshold must be attained by the total photon flow of all the laser modes. So long as the laser bandwidth is sufficiently small that all nonlinear processes are considered phase matched, then the multi-mode laser provides the same gain as a single-frequency laser of the same total power.[13]

After multiplying Eq.(6) by E_{s} and Eq.(7) by $E_{\mathrm{p}j}$, the coupled equations are obtained,

$$\tau_{\mathrm{s}}\dot{P}_{\mathrm{s}} = P_{\mathrm{s}}\left(\sum_j P_{\mathrm{p}j} - 1\right), \quad (10)$$

$$\tau_{\mathrm{p}}\dot{P}_{\mathrm{p}j} = P_{\mathrm{p}j}\left(N_j - 1 - F'P_{\mathrm{s}}\right). \quad (11)$$

Here $N_j = G_j/G_{j-\mathrm{th}}$, $P_{\mathrm{s}} = F_{\mathrm{s}}/[\sum F_{\mathrm{p}j}]_{\mathrm{th}}$, $P_{\mathrm{p}j} = F_{\mathrm{p}j}/[\sum F_{\mathrm{p}j}]_{\mathrm{th}}$ are normalized gain, signal power, and laser power respectively. $F' = \tau'_{\mathrm{p}}n_{\mathrm{s}}L_{\mathrm{s}}/\tau'_{\mathrm{s}}n_{\mathrm{p}}L_{\mathrm{p}}$ is the ratio between the laser and signal cavity finesses; τ_{s}, τ_{p} are the signal and pump photon lifetimes respectively.

The evolution equation for the saturated laser gain, which can derived from the Bloch equations[12]

$$\tau_{\mathrm{u}}\dot{N}_j = \sigma_j - N_j\left(1 + xP_{\mathrm{p}j} + x\mu\sum_{k\neq j}P_{\mathrm{p}k}\right). \quad (12)$$

Where τ_{u} is the upper-state lifetime and σ_j is the number of times for which the jth laser mode is pumped above threshold ($\sigma_j \propto$ unsaturated gain). The coefficient $\mu < 1$ relates to the cross-saturation between pairs of laser modes, x is a saturation parameter which defined as

$$x = \left[\sum F_{\mathrm{p}j}\right]_{\mathrm{th}}/F_{\mathrm{sat}}, \quad (13)$$

where F_{sat} is the laser saturation photon-flow.

2.4. Steady-state solutions

For single-frequency laser field and operation above the OPO threshold: $\sigma \geq \sigma_{\mathrm{th-OPO}} = 1 + x$, setting $t = 0$, we can get the steady-state solution from Eqs.(10)–(12) as:

$$P_{\mathrm{p}}^0 = 1, \quad N^0 = \sigma/(1+x),$$
$$P_{\mathrm{s}}^0 = (N^0 - 1)/F'. \quad (14)$$

Then consider the multi-frequency laser field, the general steady-state solutions of the Eqs.(10)–(12) with M axial laser modes are

$$P_{\mathrm{p}j}^0 = \sigma_j/\sum_j\sigma_j + (1+x\mu) \times\left(M\sigma_j - \sum_j\sigma_j\right)\Big/\left(x(1-\mu)\sum_j\sigma_j\right),$$
$$N_j^0 = \sum_j\sigma_j/\{M + x(1+\mu(M-1))\},$$
$$P_{\mathrm{s}}^0 = (N_j^0 - 1)/F'. \quad (15)$$

The requirement is $P_{\mathrm{p}j}^0 > 0$ for the operation, so each of the M modes should satisfy

$$\sigma_j \geq (\sigma_j)_{\mathrm{th-L}} = N_j^0(1+x\mu) = 1 + x\mu\sum_{k\neq j}P_{\mathrm{p}k}^0 + F'P_{\mathrm{s}}^0(1+x\mu). \quad (16)$$

The new threshold condition includes the parametric loss for individual mode. To achieve oscillation, the gain for a given laser mode must be greater than a fraction $[1+x\mu]/[M(1+x\mu)+x(1-\mu)]$ of the total laser gain.

3. Experiments and results

A schematic diagram of the intracavity SRO in the experiment is depicted in Fig.2. The pump source for the SRO was a diode-pumped CW Nd:YVO_4 laser comprising a 0.4%-doped a-cut gain crystal with dimensions of 3 mm × 3 mm × 8 mm. The Laser diode (LD) was a high-brightness fibre-coupled diode-laser-array emitting at 808 nm with a 400 μm fibre bundle end. The multi-lens optical coupler (L_1 and L_2) focused the diode laser to the Nd:YVO_4 crystal with a spot size of 400 μm in diameter. The entrance face of the Nd:YVO_4 was coated for high reflection (HR) at 1064 nm and antireflection (AR) coated at 808 nm. The output face of the Nd:YVO_4 was AR coated at 1064 nm. The Nd:YVO_4 crystal was cooled by refrigerant water at 18°C.

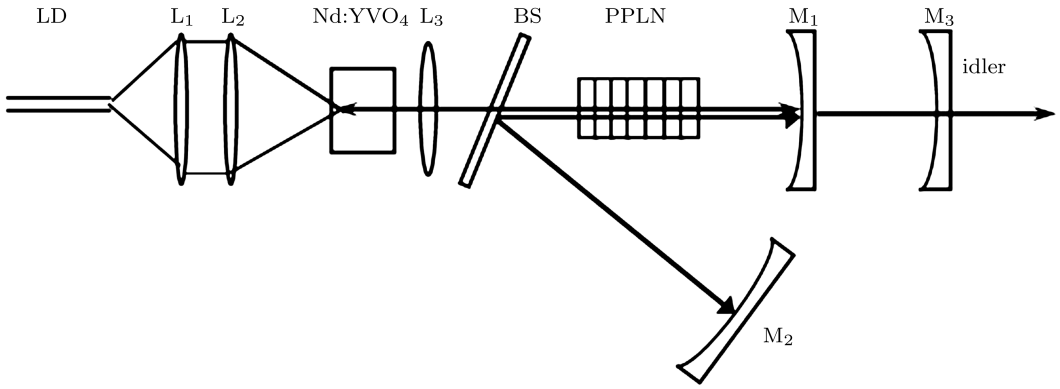


Fig.2. Schematic diagram of the all-solid-state CW intracavity SRO L_1 and L_2: coupling lens, L_3: focal lens, BS: beam splitter, M_1 and M_2: cavity mirrors, M_3:filter.

The SRO resonator consisted of a concave high reflector M_2 ($R = 200$ mm) and an output mirror M_1 (made of CaF_2, $R = 100$ mm). M_1 was a concave reflector and was HR coated ($R > 99\%$) at both the pump and the resonant signal wavelengths (1.4–1.6 μm) on concave face and was high transmission (HT) ($T > 94.6\%$) coated at the idler wavelengths (3.7–4.1 μm) on both sides. M_2 was specified to be highly reflecting ($R > 99\%$) at the signal wavelength range (1.4–1.6 μm) only. The flat-flat BS was HT coated at 1064 nm on both sides and HR at 1.4–1.6 μm on one side. An uncoated PPLN crystal with dimensions of 24 mm × 8 mm × 1 mm, which contains 7 gratings, equally spaced in periods from 26 μm to 29 μm, was employed in experiments. To facilitate temperature tuning and to avoid photorefractive effects, the PPLN crystal was placed in a servo-controlled oven. Mirror M_3 (identical with M_1) was used as a filter.

For keeping the Nd:YVO_4 laser operating at high power and better beam quality, the thermal lens effects were considered to make the Nd:YVO_4 laser operate at the tangential stable region boundary in the experiment, where the larger oscillating mode volume and the pumping mode volume matched well at the Nd:YVO_4 crystal.[14] And in order to realize an efficient OPO operation, the pump intensities in the OPO resonator should be increased and the diffraction loss of the OPO should be reduced. A lens L_3, which had a focal length of 100 mm and was coated AR at 1064 nm on both sides, was inserted into the cavity as the optical ballast to make the pumping radius vary insensitive with the thermal lens effects and focus the pump waist radius to 110 μm with the purpose of sufficient pump intensities. The PPLN crystal was placed at the beam waist of 1064 nm laser, which was 90 mm to M_1. By controlling the radius of curvature of M_2 and the distance between M_2 and M_1, the well matched mode volume is obtained when the signal beam waist radius is approximately as the 1064 nm laser's and the diffraction loss is the lowest. In the experiments, mirror M_2 with the radius of curvature of 200 mm and the near-concentric cavity were adopted for the PPLN-SRO. The distance between M_1 and M_2 was about 280 mm. The signal waist radius in the PPLN crystal was 120 μm as calculated, indicating mode volume matched well.

Figure 3 shows the wavelength of the CW PPLN-SRO at different temperatures at the grating period of 28.5 μm. Under the temperature of PPLN which varies from 383 K to 433 K in the experiment, the signal wavelength (measured by an optical spectrum analyser: Agilent 86142B) is 1.46 μm–1.47 μm, and the corresponding idler wavelength is 3.91 μm–3.83 μm. The theoretical curve and the experimental data are shown in Fig.3. Obviously, the experimental data fit the theoretical curve perfectly.

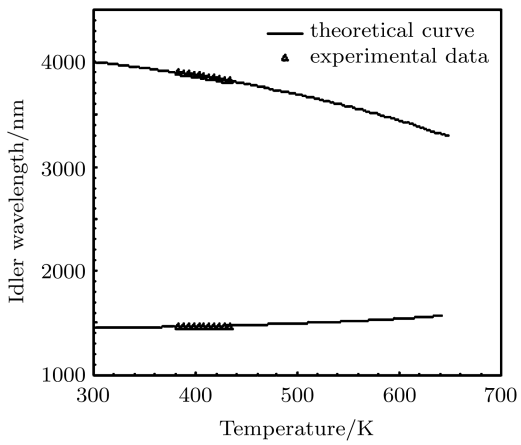


Fig.3. Wavelength of the CW PPLN-SRO as a function of temperature at grating period of 28.5 μm.

The spectra of the signal wave and the 1064 nm pump laser at the temperature of 413 K were shown in Fig.4. The signal wavelength was 1.469 μm, and the corresponding idler wavelength must be 3.86 μm as shown in Fig.3 (limited by the range of the optical spectrum analyser, the idler wavelength could not be measured). In addition, the sum-frequency-mixing wave of the signal and the pump laser at 617 nm was also found in the experiment.

Figure 5 shows the idler power (measured by a power meter: Molectron EPM1000) and the conversion efficiency at 3.86 μm as a function of diode laser power delivered to the Nd:YVO_4 crystal. For measuring the idler power precisely, a filter M_3 (made of CaF_2, HT at 3.7–4.1 μm, HR at 1064 nm and at 1.4–1.5 μm) was placed behind the output mirror M_1. The SRO threshold was 2.1 W at diode pumping power. At the LD power of 8.5 W, the maximum idler output power of 155 mW at 3.86 μm was achieved, corresponding to an optical-to-optical conversion efficiency of 1.82%.

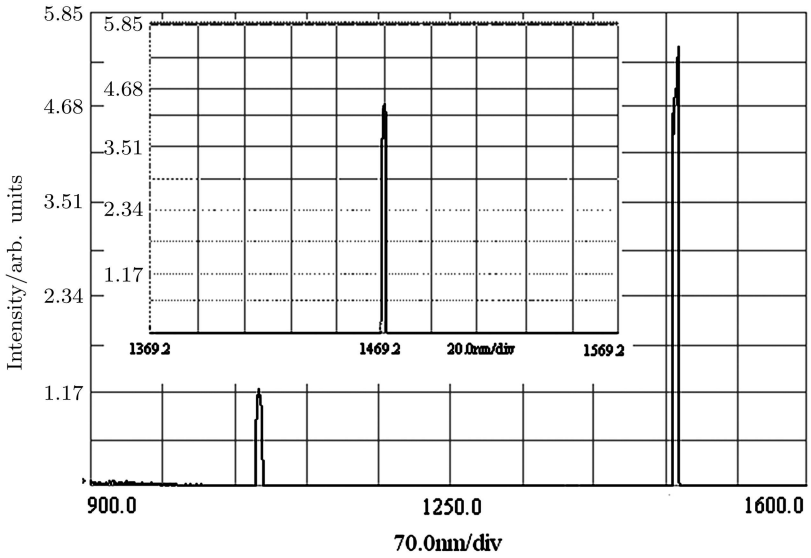


Fig.4. The spectra of the signal wavelength at 1469 nm and the pump wavelength at 1064 nm.

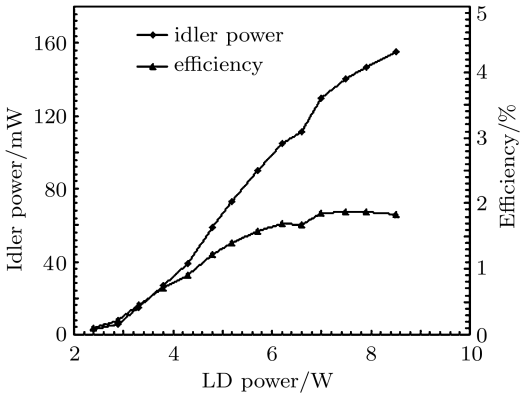


Fig.5. Output power and the conversion efficiency of the idler wavelength at 3.86 μm.

Due to the Nd:YVO_4 laser's thermal lens effects and pump depletion during the nonlinear parametric process, the instability of the idler output power was about ±8% in the experiment.

4. Conclusion

In this paper, we have demonstrated an intracavity CW PPLN—SRO pumped by a LD pumped Nd:YVO_4 laser which can generate CW mid-infrared wave. The operation of the intracavity SRO based on the multi-frequency laser field was theoretically analysed. An optical ballast lens and the near-concentric cavity were adopted by considering the thermal focal length of the Nd:YVO_4 laser. At the PPLN's grating period of 28.5 μm and the temperature of 140°, the SRO threshold is only 2.1 W, and the maximum idler output power of 155 mW at 3.86 μm is achieved at LD power of 8.5 W, leading to the optical-to-optical conversion efficiency of 1.82%.

References

[1] Phua P B, Tan B S, Wu R F, Lai K S, Chia L and Lau E 2006 *Opt. Lett.* **31** 489

[2] Lindsay I D, Stothard D J M, Rae C F and Dunn M H 2003 *Optics Express* **11** 134

[3] Carleton A, Stothard D J M, Lindsay I D, Ebrahimzadeh M and Dunn M H 2003 *Opt. Lett.* **28** 555

[4] Conroy R S, Rae C F, Dunn M H, Sinclair B D and Ley J M 1999 *Opt. Lett.* **24** 1614

[5] Stothard D J M, Ebrahimzadeh M and Dunn M H 1998 *Opt. Lett.* **23** 1895

[6] Bosenberg W R, Drobshoff A, Alexander J I, Myers L E and Byer R L 1996 *Opt. Lett.* **21** 713

[7] Lavi R, Englander A and Lallouz R 1996 *Opt. Lett.* **21** 800

[8] Lin X C, Kong Y P, Zhang Y, Zhang J, Yao A Y, Bi Y, Sun Z P, Cui D F, Li R N, Wu L A and Xu Z Y 2004 *Chin. Phys.* **13** 1042

[9] Lin X C, Bi Y, Yao A Y, Kong Y P, Zhang Y, Sun Z P, Li R N, Cui D F, Xu Z Y and Li J 2003 *Chin. Phys. Lett.* **20** 1074

[10] Turnbull G A, Dunn M H and Ebrahimzadeh M 1998 *Appl. Phys.* B **66** 701

[11] Colville F G, Dunn M H and Ebrahimzadeh M 1997 *Opt. Lett.* **22** 75

[12] Debuisschert T, Raffy J, Pocholle J P and Papuchon M 1996 *Opt. Soc. Am.* B **13** 1569

[13] Harris S E 1966 *IEEE J. Quantum Electron.* **QE-2** 701

[14] Wu D E, Zhou R, Zhang X H, Ding X, Yao J Q, Yan C F and Zhang G Y 2006 *Acta Phys. Sin.* **55** 1196 (in Chinese)